The budding yeast heterochromatic SIR complex resets upon exit from stationary phase

Hrvoje Galic[1,2], Pauline Vasseur[1,2,3] and Marta Radman-Livaja[1,2*]

[1] *Institut de Génétique Moléculaire de Montpellier, UMR 5535 CNRS, 1919 route de Mende, 34293 Montpellier cedex 5, France;*

[2] *Université de Montpellier, 163 rue Auguste Broussonnet, 34090 Montpellier, France.*

[3] *current address* : *CIRAD, Campus international de Baillarguet, UMR 117- ASTRE "Animal, Santé, Territoires, Risques & Écosystèmes", TA A-117/E, Bât. G bureau 212, 34398 Montpellier cedex 5, France*

*Corresponding author

Abstract

The budding yeast SIR complex (Silent Information Regulator) is the principal actor in heterochromatin formation, which causes epigenetically regulated gene silencing phenotypes. The maternal chromatin bound SIR complex is disassembled during replication. Consequently, if heterochromatin is to be restored on both daughter strands, the SIR complex has to be reformed on both strands to pre-replication levels. The dynamics of SIR complex maintenance and re-formation during the cell-cycle and in different growth conditions are however not clear. Understanding exchange rates of SIR subunits during the cell cycle and their distribution pattern to daughter chromatids after replication has important implications for how heterochromatic states may be inherited and therefore how epigenetic states are maintained from one cellular generation to the next. We used the tag switch RITE system to measure genome wide turnover rates of the SIR subunit Sir3 before and after exit from stationary phase and show that maternal Sir3 subunits are completely replaced with newly synthesized Sir3 at subtelomeric regions during the first cell cycle after release from stationary phase. The SIR complex is therefore not "inherited" and the silenced state has to be established *de novo* upon exit from stationary phase. Additionally, our analysis of genome-wide transcription dynamics shows that precise Sir3 dosage is needed for the optimal up-regulation of "growth" genes during the first cell-cycle after release from stationary phase.

Introduction

Budding yeast heterochromatin is a repressive structure located at the silent mating type loci (*HMR* and *HML*), telomeres and rDNA repeats. The essential component of the structure is the non-histone protein complex SIR (Silent Information Regulator), which consists mainly of Sir2, Sir3 and Sir4. Sir4 scaffolds the complex while Sir2 functions as an NAD-dependent H4K16 deacetylase, providing a high-affinity binding site for Sir3 which recruits Sir4 and so on (for review see (Grunstein and Gasser 2013)). In the classical polymerization model, SIR components are first recruited to silencer regions by a combination of silencer-binding factors (ORC –Origin Recognition Complex, Rap1 and Abf1). The SIR complex then spreads from the nucleation site (silencer) through cycles of deacetylation and nucleosome binding, which continue until the SIR complex reaches boundary elements that prevent unwanted spreading to transcriptionally active regions (for review see (Gartenberg and Smith 2016)). For example, one well-characterized boundary element is the threonine tRNA gene in the telomere-proximal region of HMR (Donze and Kamakaka 2001). Recent studies have shown that the SIR complex can also be recruited to unconventional binding sites, including tRNA genes. SIR binds to these sites mostly during genomic replication. Since these loci are tightly bound by non-histone proteins such as transcription factors which may cause replication fork stalling, it has been proposed that SIR may play a role in releasing stalled forks or preventing fork stalling (Dubarry et al. 2011; Nikolov and Taddei 2016).

It has been shown that over-expressed Sir3p can be incorporated into existing heterochromatin(Cheng and Gartenberg 2000). However, beyond this bulk measurement, the locus-specific dynamics of the chromatin bound SIR complex within and from one cell generation to another have not yet been measured. How heterochromatic SIR complexes exchange their components during the cell cycle and how they are distributed to daughter chromatids after replication has important implications for how heterochromatic states are maintained and whether they may be inherited. The maternal SIR complex has to be disassembled during replication and if heterochromatin is to be restored on both daughter strands, the SIR complex has to be reformed on both strands to pre-replication levels.

Another open question is how chromatin bound complexes that epigenetically determine gene expression states, like the SIR complex, respond to environmental challenges such as nutrient depletion. Indeed, under unfavorable conditions, yeast cells stop growing and enter the stationary phase, which lasts until depleted nutrients are restored. Molecular hallmarks of the stationary phase include transcriptional reprogramming, spatial reorganization of the genome and a 300-fold decrease in protein synthesis rates(McKnight et

al. 2015). While the organization of the SIR complex in stationary phase has been described, the dynamics of the SIR complex during and following exit from the stationary phase are still poorly understood(Guidi et al. 2015). These questions have motivated us to investigate the dynamics of the SIR complex during and upon release from the stationary phase. Our strategy was to use the Recombination-Induced Tag Exchange (RITE) method(Verzijlbergen et al. 2010; Terweij et al. 2013) to map genome wide Sir3 turnover rates with the goal to better understand the mechanisms of heterochromatin maintenance and find out whether the SIR complex is "inherited" on newly replicated daughter chromatids. We chose to focus on the Sir3 subunit because Sir3 is the limiting factor that determines the extent of SIR complex polymerization and the location of SIR complex boundaries.(Renauld et al. 1993; Hecht et al. 1996; Radman-Livaja et al. 2011)

Our results show that during stationary phase, subtelomeric Sir3 occupancy is reduced 4-fold and Sir3 turnover is undetectable. Sir3 bound to chromatin is then completely replaced with newly synthesized Sir3 subunits at the end of the first cell cycle upon release from stationary phase, suggesting that at least the Sir3 subunit of the SIR complex is not inherited and therefore does not contribute to the epigenetic inheritance of the silenced state in these conditions. Heterochromatic complexes are instead completely "reset" after exit from quiescence. Additionally, average Sir3 occupancy at subtelomeric loci decreases rapidly before the first cell division after release from stationary phase and then increases gradually over multiple cell divisions. We propose that the observed transient instability of the SIR complex after release from stationary phase is a functional adaptation that allows the cell to rapidly respond to changing growth conditions and upregulate genes involved in carbon source metabolism and cellular growth.

Results

Sir3 subunit exchange dynamics during and after release from stationary phase

We used the RITE tag switch system developed by Fred van Leeuwen(Verzijlbergen et al. 2010) to construct the Sir3 "tag switch" module. The genomic *Sir3* locus was engineered with a C-terminal tag switch cassette containing loxP sites, and the HA and T7 tags, separated by a transcription termination signal, and the hygromycin resistance gene (**Figure 1A**). The host strain carries the CreEBD78 recombinase, which is activated upon estradiol addition. After Cre-mediated recombination of LoxP sites, the HA tag on Sir3 is switched to the T7 tag. Recombination efficiency is assessed by growth on hygromycin plates, and is typically ~97% if arrested cells are treated with estradiol for at least 16hrs.

Cells were grown in glucose rich medium (YPD) for 48hrs until they reached the stationary phase. Since it has been shown that after 48hrs the majority of cells in the

population have the characteristics of quiescent cells i.e. the ability to retain viability and reproductive capacity in the absence of nutrients, we consider that our experiments record the average behavior of quiescent cells upon exit from stationary phase(Allen et al. 2006). Stationary phase cells were incubated with estradiol for 16hrs to induce the Cre mediated tag switch. Anti-HA (old Sir3) and anti-T7 (new Sir3) chromatin immuno-precipitations were performed in parallel at regular intervals before and after Cre activation. Formaldehyde cross-linked chromatin was sonicated to 300-500bp fragments before immune precipitation and DNA isolated from immune-precipitated chromatin fragments was analyzed with deep-sequencing.

ChIP-seq of old and new Sir3 showed that Sir3 dynamics are similar at all heterochromatic loci, including silent mating type loci and subtelomeric regions (**Figure 1 B-C, E-F**). Namely, the old Sir3 is maintained in stationary phase cells even after the tag switch, although overall Sir3 occupancy is decreased 4 fold compared to the pre-stationary midlog phase (**Supplementary Figure S1 B-C)**. After release into fresh media old Sir3 completely disappears at the time of the first cell doubling and is replaced by new Sir3. New Sir3 enrichment is however still low even after the twelfth doubling: 3 fold lower than old Sir3 immediately after release and ~7 fold lower than Sir3 in mid-log cells (Radman-Livaja et al. 2011) (**Figure 1 B-C and Supplementary Figure S1 B-C**). While the differences in Sir3 enrichment levels between new Sir3 after several divisions following the exit from stationary phase and old Sir3 in mid-log before stationary phase could be due to differences in binding affinities of the anti-T7 (new Sir3) and anti-HA (old Sir3) antibodies to their respective epitopes, it is nevertheless apparent that new Sir3 binding to subtelomeric loci does not reach saturation even after several doublings. The observed pattern of Sir3 binding dynamics in cell populations after exit from stationary phase suggests that the existing Sir3 is rapidly removed from chromatin when cells resume growth before the first cell division and is gradually replaced with new Sir3 over several cell division cycles. Interestingly, Sir3 replacement at silent mating type loci is faster than at subtelomeric loci and new Sir3 occupancy reaches a plateau after 1-3 doublings, probably as a consequence of the stronger SIR complex nucleation capacity of HML and HMR silencers compared to subtelomeric silencers (**Figure 1 E-F, Supplementary Figure S1 E-F**).

Sir3 removal, heterochromatin instability and "growth" genes up-regulation upon release from stationary phase

The SIR complex appears to be unstable in the first cell cycle after exit from stationary phase, thus making heterochromatin potentially permissive to transcription during that period. The rapid decrease in chromatin occupancy of old Sir3 during the first cell cycle

after release coincides with a fast decline in total cellular old Sir3 levels resulting in the complete disappearance of old Sir3 by the time of the first cellular doubling accompanied by a slow and gradual increase in new Sir3 which starts around 90min after release (**Figure 2A**). Since the rapidly declining levels of old Sir3 and the slow synthesis of new Sir3 could compromise heterochromatin function we tested the silencing potential of SIR complexes after exit from stationary phase using the "α-factor test", described below (**Figure 2B**).

MATa (Mating Type a) cells will respond to the presence of α-factor (mating pheromone α) by arresting in G1 and forming a "shmoo" if the silent mating type locus *HML* (containing the genes for mating type α) is stably heterochromatinized with the SIR complex. If *HML* is not fully silenced, cells will behave like pseudo-diploids and will not respond to α-factor. Log-phase cells should therefore predominantly respond to α-factor and become shmoo. On the other hand, we expect that populations exposed to α-factor immediately upon exit from quiescence will have a higher fraction of cells that form buds. This is exactly what we observe: there are ~two times more cells that divide and don't form shmoon in populations exiting stationary phase than in mid-log populations. If cells are allowed to divide even just once after release and are then exposed to α-factor they arrest normally and form stable "shmoon" like mid-log cells (**Figure 2B**). The inability to form shmoon in a subpopulation of cells exiting quiescence is not due to a Sir3 independent defect since cells that can shmoo in log phase in the absence of α-factor irrespective of the presence Sir3 due to a *HMLα/MATa* double deletion, also shmoo with 100% efficiency upon release from stationary phase even in the absence of Sir3 (**Figure 2C**). The transient decrease in Sir3 amount at subtelomeric regions during the first cell cycle upon exit from quiescence can however be overcome with Sir3 overexpression (**Figure 3**). In a galactose inducible overexpression system, Sir3 occupancy starts increasing immediately upon release of stationary cells into galactose even before the first cell division, suggesting that SIR complex renewal does not directly depend on DNA replication or cell division but is likely driven by the rate of accumulation of newly synthesized Sir3. Overexpression of Sir3 can therefore compensate for the rapid removal of old Sir3 that was bound to chromatin in stationary phase. It is however important to note that the process of old Sir3 removal occurs independently of Sir3 synthesis as evidenced by the complete disappearance of chromatin bound old Sir3 by the second doubling upon release into dextrose or raffinose in which new Sir3 is not expressed (**Figure 3 F, N**). In other words, the removal of old Sir3 from chromatin is not "driven" by its replacement with new Sir3.

We have also tested the effects of Sir3 dynamics during the stationary to growth phase transition on genome wide gene expression levels. Changes in mRNA enrichment relative to a genome-wide average in the wt Sir3 (strain used in Figures 1 and S1), Sir3Δ or

oeSir3 (used in Figure 3) strains show that wt Sir3 levels are needed to maintain the up-regulation of 710 genes during the first cell cycle after release from stationary phase (**Figure 4**). The up –regulated genes are enriched for "growth" genes involved in ribosome synthesis, mitochondrial processes and amino-acid and carbon metabolism (Table S1). These genes are all upregulated in stationary phase but their expression starts to decrease immediately after release from stationary phase either in the absence of Sir3 (Sir3Δ strain) or in the presence of excess total Sir3 (oe Sir3 strain). In wt cells on the other hand, they are further upregulated immediately after release and their mRNA levels stay high until the first division when they drop abruptly down to approximately mid-log levels (**Figure 4C-D**). An analysis of median Sir3 enrichment in the coding regions of these genes suggests that the observed transcription up-regulation may be a direct consequence of low level Sir3 enrichment at these genes (**Figure 4 E**). The observed Sir3 enrichment values are relative to average genome-wide Sir3 enrichment in each time-point since our ChIP-seq experiments were not normalized to a spike-in control. Even though we cannot measure absolute changes in Sir3 occupancy at these genes, we do detect a trend in relative Sir3 occupancy upon release from stationary phase. The median Sir3 enrichment over the time course is proportional to transcription levels with the highly expressed cluster 1 having the highest Sir3 occupancy, as has been documented before (Radman-Livaja et al. 2011). Unlike at subtelomeric regions where old Sir3 levels decrease abruptly immediately after release, old Sir3 enrichment at induced genes appears to be mostly constant although with a slight drop immediately after release in clusters 2 and 3 (**Figure 4E**). On the other hand Sir3 dynamics after the first cell division are similar on subtelomeric regions and on these "growth" response genes: the exchange of old Sir3 subunits with new Sir3 starts with the first cell division after release with similar rates as in subtelomeric regions (**Figure 4 F-G**). When Sir3 is over-expressed however, Sir3 enrichment drops immediately after release (except for cluster 1 where there is an initial increase 1hr after release) and continues to decrease with each cell division. Since Sir3 enrichments are calculated relative to a genome-wide average, the apparent depletion of Sir3 at these genes is a consequence of Sir3 accumulation in subtelomeric regions after release and its spreading beyond heterochromatin boundaries found in wt cells (compare Figures 1B and 3B). The correlation between relative Sir3 depletion and impaired up-regulation of "growth" response genes in cells with over expressed Sir3 as well as the correlation between constant Sir3 occupancy and up-regulation of these same genes in wt cells, suggest that controlled and potentially transcription dependent Sir3 binding may have a direct effect on gene expression.

Sir2 binding during and after release from stationary phase

Genome-wide Sir2 binding dynamics during the stationary to growth phase transition are similar to Sir3 dynamics with some quantitative differences as shown in **Figure 5**. Like for Sir3, we observe a decrease in Sir2 occupancy at subtelomeres, silent mating type loci and rDNA in stationary phase, although the decrease is more modest: 50% (silent mating type loci; **Figure 5E-F**) to ~2 fold (subtelomeric regions, **Figure 5C** and rDNA, **Figure 5G**). Also, the return to (subtelomeric regions) or even above pre-stationary phase levels (silent mating type loci and rDNA) is observed immediately after the first cell division after release, while Sir3 has not reached saturation even after 12 doublings.

Sir3 and Sir2 binding to tDNA

Our results have unexpectedly uncovered non-canonical Sir3 binding to tRNA genes (**Figures 1D, S1D, 3G-J**). New, T7 tagged Sir3 is significantly enriched at all but 20 tRNA genes immediately upon release from stationary phase and this high Sir3 occupancy persists at least for 5 subsequent doublings (**Figure 1D**). The source of the gradual increase in Sir3-HA binding to tRNA genes is likely originating from the fraction of cells (~2.5%) that did not complete the tag switch. A replicate experiment using a different anti-T7 antibody (a monoclonal one versus the polyclonal one in Figure 1) does confirm Sir3-T7 binding to tDNAs upon release (**Figure S1 D**) but with Sir3 enrichment levels that are 8 to 16 fold lower than with the polyclonal antibody used in Figure 1. Unlike their dynamics at subtelomeric loci, new Sir3-T7 and old Sir3-HA in the replicate experiment seem to follow the same binding dynamics with the same level of occupancy: no binding during the stationary phase followed by a "jump" in occupancy after the first doubling and constant binding for at least twelve doublings afterwards. The discrepancies in Sir3-T7 enrichment at tDNAs between the two replicates are puzzling and are possibly a consequence of different affinities of the polyclonal and the monoclonal antibodies for the T7 epitope in the context of different Sir3 configurations found at tDNAs and subtelomeres. The monoclonal and the polyclonal anti-T7 antibodies seem to bind with comparable efficiency to Sir3 when it is present in multiple subunits in the densely packaged configuration of a SIR polymer at subtelomeric and silent mating type loci. The polyclonal anti-T7 is on the other hand more efficient than the monoclonal antibody when Sir3 stoichiometry is low as it is likely to be at tDNAs.

The signal clearly correlates with Sir3 presence in the cell: 1. only Sir3-HA is detected in midlog cells before the tag switch from HA to T7, while Sir3-T7 and Sir3-HA are both detected after release from stationary phase following the tag switch (Figure S1 D, the Sir3-HA signal comes probably from cells that did not recombine the two tags); 2. The Sir3-HA signal from the Sir3 overexpression system is undetectable in the 12th doubling after release into dextrose or raffinose media where Sir3 is not expressed while it is still there in

the 12th doubling after release into galactose when Sir3 is overexpressed (Figure 3G-J). Consequently, the enrichment of tDNA sequences in our Sir3 ChIP-seq datasets cannot be due to non-specific binding of these sequences to antibodies or protein A beads as has been proposed previously(Teytelman et al. 2013), nor is it likely to be a tag artefact since tDNA sequences were isolated with the anti-HA (Figures 1D, S1D, and 3G-J) and the anti-T7 antibodies (Figures 1D, S1D). We cannot, however exclude the possibility that Sir3 binding to tDNAs has no biological significance and is merely a consequence of transient and non-specific "stickiness" of nucleoplasmic Sir3 to tDNA sequences in vivo or even after cell fixation.

Sir2 also binds to tDNAs although the binding pattern and kinetics are somewhat different from Sir3. While Sir3 occupies a footprint from -100bp to 200bp around the start of the tRNA gene throughout the time course, Sir2's footprint spreads progressively from +-150bp around the tRNA gene start in the first cell cycle to +-400bp by the 12th cycle (compare the top panels of Figures 1D, S1D and 5D). Also, while the position of peak binding immediately downstream of the tRNA gene start is common to both Sir3 and Sir2, the rate of peak height changes is different for the two proteins. Peak height already reaches a plateau after the first cell cycle for Sir3, while it is still growing (although slowly) after the 12th doubling for Sir2 (**Figure 6D**). The timing of the binding signals and the footprint patterns of the two proteins suggest that Sir3 might be binding first and might then recruit Sir2 which then spreads to the nucleosomes immediately adjacent to the tRNA gene.

It is curious that the enrichment signal at tDNAs disappears in stationary phase for both Sir3 tag switch replicates and in the Sir3 overexpression system as well as Sir2 (Figures 1D, S1D, 3G-J and 5D, respectively) even though Sir3 and Sir2 still bind to silent mating type loci and subtelomeric regions although at reduced levels, and may reflect the scarcity of nucleoplasmic Sir3 and possibly Sir2 in stationary cells. The fluctuations in Sir3 occupancy at tDNAs coincide with changes in growth conditions: 1.low level binding in mid-log (Figure S1D); 2. no binding in stationary phase; 3. increased binding upon release from stationary phase that reaches a plateau after the first cell division and stays higher than the previous midlog phase even twelve doublings after release from stationary phase. This suggests that Sir3 binding may be linked to changes in the chromatin configuration and/or gene expression state of tRNA genes.

TFIIIC is a transcription factor responsible for the recruitment of the RNApolIII transcription machinery and its binding sites are verified heterochromatin boundary and chromatin insulator elements(Simms et al. 2008). We therefore mapped the TAP-tagged TFC3 (a subunit of TFIIIC) genome wide binding pattern upon release from stationary phase

to find out whether there is a correlation between TFIIIC and Sir3 binding to tDNAs (**Figure 6**).

We have identified three tRNA gene clusters with specific TFIIIC binding dynamics (**Figure 6B-C**). Sir3 and Sir2 binding dynamics correlate with TFIIIC binding in less than 50% of all tRNA genes (124 tRNA genes in cluster 1 out of a total of 273 tRNA genes) (**Figure 6 D-F**). Consequently Sir3 and Sir2 are not likely to bind to tDNAs in response to tRNA gene activation but they may be "recognizing" structural chromatin features common to all tRNA genes independently of their gene expression state.

Discussion

Our results suggest that yeast heterochromatin is reprogrammed upon exit from stationary phase. We observe a ~4 fold and ~2 fold drop in Sir3 and Sir2 subtelomeric occupancy, respectively, when cells enter the stationary phase that is followed by an even steeper drop of Sir3 occupancy during the first cell cycle after release from stationary phase. All Sir3 proteins bound to subtelomeric and silent mating type loci are replaced with newly synthesized Sir3 after the first division following release. Surprisingly, the enrichment of new Sir3 subunits in subtelomeric regions increases slowly and appears to not reach saturation even after 12 cell divisions. Even though we have not measured Sir2 turnover rates, our Sir2 ChIP-seq time-course experiment clearly shows that Sir2, unlike Sir3, comes back to pre-stationary levels by the first cell division after release, suggesting that heterochromatin function is potentially regulated by modulating Sir3 dosage. Further experiments will be necessary to understand how the differences in the stoichiometry of Sir2 and Sir3 in this "reset" form of heterochromatin in which Sir2 levels are constant and Sir3 gradually increases over multiple cell generations affect the functionality and stability of heterochromatin.

The biological significance of this kind of heterochromatic "clean slate" upon exit from quiescence and the slow rebuilding of heterochromatin structure is not clear. The apparent depletion of Sir3 before the first cell division after release can be overcome with Sir3 overexpression, bringing up the possibility that the naturally limiting amount of Sir3 has a regulatory function. It opens up the question of the function of Sir3 stoichiometry at heterochromatic loci. Are there different higher order conformations of heterochromatin that depend on the amount of Sir3 and does heterochromatin that contains less Sir3 have greater plasticity that would facilitate the cell's response to environmental changes and stressful growth conditions?

Sir3 appears to be actively kept at low levels in the first two divisions after release as our Western blot results suggest, even though global protein synthesis is greatly increased (for review see(Valcourt et al. 2012)). Heterochromatin formation may be impaired to potentially prevent mating during first divisions when the cell is replenishing its protein content or to allow expression of subtelomeric genes or both. Sir3 also becomes hyperphosphorylated in stress conditions, such as nutrient depletion, following the inactivation of the TOR pathway(Stone and Pillus 1996). Sir3 hyperphosphorylation in turn causes the derepression of subtelomeric PAU genes involved in cell wall restructuring (Ai et al. 2002). Since TOR activity is necessary for growth, an alternative pathway to Sir3 phosphorylation that insures the expression of subtelomeric genes upon exit from quiescence may be necessary and may involve targeted degradation of Sir3 proteins and/or reduced synthesis of Sir3 proteins. A small increase in relative mRNA abundance of low expressed genes cannot be detected in our RNA-seq experiment because mRNA enrichment is normalized to average genome-wide sequencing read density. We were therefore unable to detect changes in subtelomeric gene expression that are likely to be subtle. We do detect, however, Sir3 dependent up–regulation of ~700 "growth" response genes localized throughout the genome. Indeed, a precise control of genome-wide Sir3 density upon exit from stationary phase appears to be necessary for sustained up-regulation of "growth" genes, which presumably enables optimal cell growth in the first cell cycle after release (**Figure 4**). Cells without Sir3 or with excessive amounts of Sir3 both fail to maintain high levels of up-regulation of these genes in the first cell cycle after release. Moreover, the correlation between mRNA and Sir3 levels and the specific pattern of Sir3 turnover at these genes suggest that Sir3 may play a direct role in transcription regulation. Interestingly, (Weiner et al. 2012) also proposed that Sir3 might play a direct role in the regulation of ribosomal protein gene expression during the stress. There is therefore an intriguing possibility that apparently transcription dependent low level Sir3 binding to gene bodies of environmentally responsive genes directly regulates transcription of these genes in response to environmental signals.

Our genome-wide maps of Sir3 dynamics have also unexpectedly revealed a potentially new function of the Sir complex at tDNA loci. Even though the pervasive binding of Sir3 and Sir2 to tRNA genes may be an experimental artefact with no biological function, the dynamics of Sir3 and Sir2 binding during stationary to growth phase transitions do raise some intriguing possibilities. Sir3 binding may precede TFIIIC binding to reorganize the nucleosome configuration that may have been altered in stationary phase and thus prepare tRNA genes for optimal activation. tRNA genes have a specific nucleosome organization that somewhat resembles a yeast RNApol2 gene promoter (**Supplementary Figure S2A**). There is a nucleosome free region (NFR) covering the entire tRNA gene (-100bp to 150bp around

the tRNA gene start site, datasets used for the analysis were taken from (Weiner et al. 2010; Ziane et al. 2019)) and the nucleosomes surrounding the NFR on either side are enriched for H3K56ac (a mark of newly synthesized histone H3, dataset from (Ziane et al. 2019)) and the H2A variant Htz (dataset from (Watanabe et al. 2013)), both characteristics of high nucleosome turnover rates (Dion et al. 2007). The nucleosomal organization of tRNA genes is a dynamic structure as is evident from nucleosome and H3K56ac tDNA profiles from replicating mid-log cells (Figure S2B). Replicated tRNA genes have a wider and shallower NFR that seems to be partially populated with nucleosomes (compare the MNAse-seq profiles from bulk and nascent chromatin in the left panel) and an asymmetric H3K56ac distribution with less H3K56ac downstream of the tRNA gene that is more pronounced in early S-phase compared to mid-S-phase. Thus, DNA replication disrupts chromatin organization of tRNA genes which needs to be subsequently restored. This is supported by evidence that shows that concerted activity of DNA polymerase epsilon, the H3K56 acetylase rtt109 and the chromatin remodeler Rsc is needed to create the nucleosome positioning pattern of the tRNA insulator at HMR(Dhillon et al. 2009). tRNA genes are also known "obstacles" for replication forks(Deshpande and Newlon 1996) but not all tRNA genes have the same capacity to slow forks down in optimal growth conditions(Ivessa et al. 2003). It will therefore be interesting to see whether the chromatin structure of tRNA genes is altered in stationary phase and whether the Sir complex functions to reorganize nucleosomes at tRNA genes after exit from quiescence to prevent dangerous fork stalling in the first S-phase after release and/or prime tRNA genes for transcription activation or insulator function.

Our results have revealed the dynamic nature of yeast heterochromatin that changes in response to environmental challenges that cells face in variable growth conditions. Future studies should explore the regulatory mechanisms that ensure heterochromatin plasticity while preserving its functionality. We have also uncovered two potential new roles for Sir3: one in gene expression regulation of genes involved in the stationary to growth phase transition and the other in tDNA binding. Our study joins the growing body of work that delves into the dynamics of chromatin structure in different organisms and is yet another reminder that chromatin organization is not a static structure that reaches some sort of final stable state that just needs to be maintained once cells have differentiated. It is instead an active element in the cell's response to its environment that has to be continuously shaped and reshaped by specialized cellular processes in order to ensure the survival and preserve the function of each cell.

Materials and Methods

Yeast Strains

The strain used in Figures 1, 2, and S1 is MRL9.1 (S288C: *MATa his3d200 leu2d0 lys2d0 met15d0 trp1d63 ura3d0 bar1::HisG HIS3 Pgpd_CRE_EBD78 Sir3Histag-LoxP-3xHA-Hygro-LoxP-3xT7*) that was constructed by transforming NKI12318 (*MATa his3d200 leu2d0 lys2d0 met15d0 trp1d63 ura3d0 bar1::HisG HIS3 Pgpd_CRE_EBD78*; courtesy of Fred van Leeuwen) with the RITE-switch (*LoxP-3xHA-Hygro-LoxP-3xT7*) cassette amplified from the pFvL159 plasmid (Fred van Leeuwen) with primers (
forward:
5'GCCTTTTCGATGGATGAAGAATTCAAAAATATGGACTGCATTCATCACCATCAC CATCACGGTGGATCTGGTGGATCT;
reverse:
5'CATAGGCATATCTATGGCGGAAGTGAAAATGAATGTTGGTGGTGATTACGCCA AGCTCG) compatible for homologous recombination with the C-terminal end of the Sir3 gene. Cassette incorporation was verified by PCR.
The Sir3 over-expression strain in Figure 3 is THC70 (W303: *MATa HMLa HMRa ade2-1 can1-100 his3-11,15 leu2-3,112 trp1-1 matΔ::TRP1 hmr::rHMRa hmlΔ::kanMX ura3-1::GAL10P–Sir3HA::URA3 bar1Δ::hisG lys2Δ sir3Δ::HIS3*) (courtesy of K.Struhl (Cheng and Gartenberg 2000; Katan-Khaykovich and Struhl 2005)). TAP-tagged Sir2 (YDL042C) and TFC3 (YAL001C, subunit TFIIIC) (S288C: *MATa his3Δ1 leu2Δ0 met15Δ0 ura3Δ0 ORF-TAP:HIS3MX6*) strains were both obtained from the yeast TAP-tagged ORF library (Dharmacon). The Sir3D strain from Figure 6 is MRL5.1 (S288C: *MATa ura3D leu2D his3D met15D sir3D:KANR*).

Cell culture

Sir3 tag exchange time course:

All cultures were incubated at 30˚C in an incubator shaker at 220 rpm, crosslinked for 20 min with 1% formaldehyde and quenched for 5 min with 125mM Glycine, unless indicated otherwise. Two 10 ml cultures were grown overnight in YPD (2% glucose). One culture contained hygromicin (0,3 mg/mL; the Hyg+ culture). Hyg+ and Hyg- saturated cultures were then transferred to flasks with 90 ml YPD and hygromicin was added to the Hyg+ culture and incubated for 24h until glucose was depleted and they entered the stationary phase. A 20 ml aliquot from the Hyg+ culture was fixed, pelleted and flash frozen in liquid nitrogen and kept at -80°C as the "before switch" stationary phase sample. The rest of the Hyg+ and Hyg- cultures were pelleted and 80 ml of the Hyg- supernatant was used to resuspend the Hyg+ pellet, and the Hyg+ supernatant and Hyg- pellet were discarded. The resuspended 80 ml culture was inoculated with 1 μM estradiol (Sigma) in order to induce tag exchange, and and incubated overnight for at least 16h. An aliquot for the "after switch" stationary phase sample was processed as above. The remaining culture was diluted to OD 0.3

with fresh YPD (total volume: 1600-2000 ml) and incubated at 30°C to release the culture from stationary phase. 400 ml aliquots were taken at 0, 30 and 1h 30 min after release and after indicated cell doublings (monitored by OD measurements; the first doubling typically takes place 3.5 hours after release and each subsequent doubling takes 1.5hrs). Aliquots for each time point were processed as above and fresh YPD was added to the rest of the culture in order to keep cell density constant (constant OD) maintain cells in exponential growth.

Small cell aliquots (50ul of from a 1:100000 dilution) before and after tag switch were plated on YPD plates and replica-plated on YPD+hygromycin to estimate recombination efficiency. The average recombination efficiency in our cell culture conditions is 96.9% (from 11 independent experiments).

Sir2-TAP and TFC3-TAP time course :

Cultures were done as above except without the Hyg+ culture and estradiol addition, and cells were released from stationary phase after a 48h incubation in YPD.

Western blot

10 mL aliquots from time points above were mixed with 2 mL 100% TCA and kept on ice for 10 min. Cells were then pelleted and washed twice with 500 µL 10% cold TCA. Pellets were resuspended in 300 µL 10% cold TCA and bead beated with Zirconium Sillicate beads (0.5 mm) in a bullet blender (Next Advance) for 3 times x 3 min (intensity 8). Zirconium beads were removed from the cell lysate by centrifugation and the entire cell lysate was washed twice with 200 µL 10% cold TCA. The cells lysate was then pelleted and re-suspended in 70 µL 2xSDS loading buffer (125 mM Tris pH 6.8, 20% glycerol; 4% SDS, 10% β-mercaptoethanol, 0,004% bromophenol blue) preheated at 95˚C. Approximately 30 µL Tris (1M, pH 8,7) was added to each sample to stabilize the pH. Samples were heated for 10 min at 95˚C, pelleted and the soluble protein extract in the supernatant was transferred to new tubes. Protein concentrations were measured by Bradford test kit (Sigma, B6916) and 40 µg/sample was loaded on a 7% polyacrylamide SDS-PAGE gel (30:1 acrylamide/bis-acrylamide). Proteins were transferred after electrophoresis to a PDVF membrane (Bio-Rad, 1620177). The membrane was incubated for 1h at room temperature with either anti-HA (Abcam, ab9110 (lot# GR3245707-3)) or anti-T7 (Bethyl A190-117A (lot# A190-117A-7)) antibodies to detect Sir3 and anti-α-tubulin (Sigma T6199 (lot#116M48C2V)) to detect the α-tubulin loading control. Secondary goat anti-rat-HRP (Santa Cruz Biotechnology G2514), goat anti-rabbit-HRP (Santa Cruz Biotechnology sc-2054) and bovine anti-mouse-HRP (Santa Cruz Biotechnology sc-2375) were added after the corresponding primary antibody and incubated for 1h at room temperature. All antibodies (primary and secondary) were diluted 1/10000 in 5% milk/TBS. The membrane was washed 3x in 1xTBS-10%Tween after each antibody incubation step. The blot was then covered with 500 µL Immobilon Forte

Western HRP substrate (Millipore WBLUF0500) for 2 min and protein bands were detected on a high-performance chemiluminescent film (Amersham 28906837).

Microscopy and image analysis

Cells were grown as above and concentrated by centrifugation. 3ul of the cell pellet was injected under the 0.8% agarose/YPD layer that had been poured into each well of an 8-well glass bottom microscopy plate (BioValley).

We used a wide field inverted microscope for epifluorescence and TIRF acquisition (Nikon) under the HiLo setting, with a 60X water objective with a water dispenser, and a EMCCD Evolve 512 Photometrics camera (512*512, 16µm pixel size). The time courses on growing cells were performed at 30°C. Pictures in bright field (Exposure time= 300ms and the Hilo angle= 62°) were taken every 10 or 20min for 6.5hrs.

Shmoon and budding cells were counted manually using the Image J software for visualization.

Chromatin Sonication

Cross-linked frozen cell pellets were re-suspended in 500 µL cell breaking buffer (20% glycerol, 100 mM Tris pH 7.5, 1xEDTA-free protease inhibitor cocktail (Roche)). Zirconium Sillicate beads (400 µL, 0.5 mm) were then added to each aliquot and cells were mechanically disrupted using a bullet blender (Next Advance) for 5 times x 3 min (intensity 8). Zirconium beads were removed from the cell lysate by centrifugation and the entire cell lysate was subject to sonication using the Bioruptor-Pico (Diagenode) for 3x10 cycles of 30 seconds ON/OFF each for a 500bp final median size of chromatin fragments. Cellular debris was then removed by centrifugation and the supernatant was used for ChIP.

ChIP

All steps were done at 4˚C unless indicated otherwise. For each aliquot, Buffer L (50 mM Hepes-KOH pH 7.5, 140 mM NaCl, 1 mM EDTA, 1% Triton X-100, 0.1% sodium deoxycholate) components were added from concentrated stocks (10-20X) for a total volume of 0.8 ml per aliquot. For anti-Ha and anti-T7 ChIP, each aliquot was rotated for 1 hour with 100 µL 50% Sepharose Protein A Fast-Flow bead slurry (IPA400HC, Repligen) previously equilibrated in Buffer L. The beads were pelleted at 3000 X g for 30sec, and approximately 200 µl of the supernatant was set aside for the input sample. The reminder (equivalent to 200 ml of cell culture of 0.5 OD) was separated into anti-HA and anti-T7 fractions. 10 µL anti-HA (Abcam, ab9110 (lot# GR3245707-3) and 10 µL polyclonal anti-T7 (Bethyl A190-117A (lot# A190-117A-7) (Figure 1) or 10 µL monoclonal anti-T7 (Cell Signaling Technology, DSE1X (lot#1)) (Supplementary Figure S1) were added to the corresponding aliquots.

Immunoprecipitation, washing, protein degradation, and DNA isolation were performed as previously described (Liu et al., 2003).

Purified DNA was treated with RNAse A (Qiagen) (5µg per sample 1hr at 37°C) and purified once more with Phenol-Chloroform. Purified fragments were used for NGS library construction (Input, ChIP) and subsequent NGS library construction.

For anti-TAP ChIP, aliquots were incubated directly with 10 µL anti-TAP antibodies (Thermo Scientific, CAB10001 (lot# TA261224) overnight with rotation. 50 µL of Dynabeads protein G (Thermo Scientific, 30 mg/mL) were added to each aliquot and incubated for 2h. All the following steps were as above with the following modifications: cross-links were removed after DNA elution, with a 65°C overnight incubation without proteinase K. After RNAse A treatment as above, 1mg/ml of proteinase K was added for 2hrs ate 65°C. DNA was purified with Phenol-Chloroform and further processed as above.

Cell culture and RNA isolation for RNA-seq

MRL9.1 (Sir3wt) and MRL5.1 (Sir3D) were grown as above in YPD and MRL9.1 was not subject to tag switching with estradiol. THC70 (oeSir3) were grown in conditions of Sir3 over-expression in YPGalactose. Cells were flash frozen in liquid N2 and total RNA was isolated from frozen cell pellets with Trizol. Frozen cell pellets were re-suspended directly in Trizol and bead beated in the Bullet Blender (Next Advance) for 4 times x3 min (intensity 8). RNA was then purified and DNAseI treated with the RNAeasy Column purification kit (Qiagen). Extracted total RNA amounts were measured on the Qubit and the Nanodrop and the quality was checked in a Bioanalyzer scan (Agilent). The RNA samples were then used for NGS library preparation using the Illumina TruSeq Stranded mRNA kit according to the manufacturer's protocol. Libraries were sequenced on the Illumina NextSeq550 (2x75bp) (Plateforme Transcriptome, IRMB, Montpellier, France).

NGS Input and ChIP library construction and Illumina sequencing

DNA fragments were blunt ended and phosphorylated with the Epicentre End-it-Repair kit. Adenosine nucleotide overhangs were added using Epicentre exo- Klenow. Illumina Genome sequencing adaptors with in line barcodes (

PE1-NNNNN: PhosNNNNNAGATCGGAAGAGCGGTTCAGCAGGAATGCCGAG

PE2-NNNNN: ACACTCTTTCCCTACACGACGCTCTTCCGATCTNNNNNT

, NNNNN indicates the position of the 5bp barcode, (IDT)) were then ligated over night at 16°C using the Epicentre Fast-Link ligation kit. Ligated fragments were amplified as above using the Phusion enzyme (NEB) for 18 PCR cycles with Illumina PE1 (AATGATACGGCGACCACCGAGATCTACACTCTTTCCCTACACGACGCTCTTCCGA

TCT) and PE2 (CAAGCAGAAGACGGCATACGAGATCGGTCTCGGCATTCCTGCTGAACCGCTCTTCCGATCT) primers (IDT). Reactions were cleaned between each step using MagNa beads. Libraries were mixed in equimolar amounts (12 to 21 libraries per pool) and library pools were sequenced on the HiSeq 2000 (2x75bp) (Illumina) at the CNAG, Barcelona, Spain or the NextSeq550 (2x75bp) (Plateforme Transcriptome, IRMB, Montpellier, France).

ChIP-seq data analysis

All analysis was done using in house Perl and R scripts available upon request.

Sequences were aligned to S. Cerevisiae genome using BLAT (Kent Informatics, http://hgdownload.soe.ucsc.edu/admin/). We kept reads that had at least one uniquely aligned 100% match in the paired end pair. Read count distribution was determined in 1bp windows and then normalized to 1 by dividing each base pair count with the genome-wide average base-pair count. Forward and reverse reads were then averaged and ChIP reads were normalized to their corresponding input reads.

The repetitive regions map was constructed by "BLATing" all the possible 70 bp sequences of the yeast genome and parsing all the unique 70bp sequences. All the base coordinates that were not in those unique sequences were considered repetitive.

RNA-seq data analysis

Reads were aligned and normalized as above. Normalized read densities for each gene were aligned by the transcription start site and divided into sense and antisense transcripts. The median read density for each gene (from the tss to the end of the coding sequence) was then determined for each transcript. Intron regions were excluded from the calculation.

Author Contributions

HG performed all the experiments except the microscopy part of the experiment in Figure 2B , which was performed by PV. MRL designed the experiments, analyzed the NGS data and wrote the manuscript with input from HG.

Acknowledgments

We thank Fred van Leeuwen and Kevin Struhl for yeast strains and plasmids. Thank you to Marta Gut and Julie Blanc from CNAG (Barcelona, Spain) and Véronique Pantesco (IRMB, Montpellier, France) for deep-sequencing services. We thank Virginie Georget (MRI, Biocampus, Montpellier) for her assistance with the microscope set-up. This work was supported by the ERC-Consolidator grant (NChIP 647618) (MRL).

References

Ai W, Bertram PG, Tsang CK, Chan TF, Zheng XF. 2002. Regulation of subtelomeric silencing during stress response. *Mol Cell* **10**: 1295-1305.

Allen C, Buttner S, Aragon AD, Thomas JA, Meirelles O, Jaetao JE, Benn D, Ruby SW, Veenhuis M, Madeo F et al. 2006. Isolation of quiescent and nonquiescent cells from yeast stationary-phase cultures. *J Cell Biol* **174**: 89-100.

Cheng TH, Gartenberg MR. 2000. Yeast heterochromatin is a dynamic structure that requires silencers continuously. *Genes Dev* **14**: 452-463.

Deshpande AM, Newlon CS. 1996. DNA replication fork pause sites dependent on transcription. *Science* **272**: 1030-1033.

Dhillon N, Raab J, Guzzo J, Szyjka SJ, Gangadharan S, Aparicio OM, Andrews B, Kamakaka RT. 2009. DNA polymerase epsilon, acetylases and remodellers cooperate to form a specialized chromatin structure at a tRNA insulator. *Embo J* **28**: 2583-2600.

Dion MF, Kaplan T, Kim M, Buratowski S, Friedman N, Rando OJ. 2007. Dynamics of replication-independent histone turnover in budding yeast. *Science* **315**: 1405-1408.

Donze D, Kamakaka RT. 2001. RNA polymerase III and RNA polymerase II promoter complexes are heterochromatin barriers in Saccharomyces cerevisiae. *Embo J* **20**: 520-531.

Dubarry M, Loiodice I, Chen CL, Thermes C, Taddei A. 2011. Tight protein-DNA interactions favor gene silencing. *Genes Dev* **25**: 1365-1370.

Gartenberg MR, Smith JS. 2016. The Nuts and Bolts of Transcriptionally Silent Chromatin in Saccharomyces cerevisiae. *Genetics* **203**: 1563-1599.

Grunstein M, Gasser SM. 2013. Epigenetics in Saccharomyces cerevisiae. *Cold Spring Harb Perspect Biol* **5**.

Guidi M, Ruault M, Marbouty M, Loiodice I, Cournac A, Billaudeau C, Hocher A, Mozziconacci J, Koszul R, Taddei A. 2015. Spatial reorganization of telomeres in long-lived quiescent cells. *Genome Biol* **16**: 206.

Hecht A, Strahl-Bolsinger S, Grunstein M. 1996. Spreading of transcriptional repressor SIR3 from telomeric heterochromatin. *Nature* **383**: 92-96.

Ivessa AS, Lenzmeier BA, Bessler JB, Goudsouzian LK, Schnakenberg SL, Zakian VA. 2003. The Saccharomyces cerevisiae helicase Rrm3p facilitates replication past nonhistone protein-DNA complexes. *Mol Cell* **12**: 1525-1536.

Katan-Khaykovich Y, Struhl K. 2005. Heterochromatin formation involves changes in histone modifications over multiple cell generations. *Embo J* **24**: 2138-2149.

McKnight JN, Boerma JW, Breeden LL, Tsukiyama T. 2015. Global Promoter Targeting of a Conserved Lysine Deacetylase for Transcriptional Shutoff during Quiescence Entry. *Mol Cell* **59**: 732-743.

Nikolov I, Taddei A. 2016. Linking replication stress with heterochromatin formation. *Chromosoma* **125**: 523-533.

Radman-Livaja M, Ruben G, Weiner A, Friedman N, Kamakaka R, Rando OJ. 2011. Dynamics of Sir3 spreading in budding yeast: secondary recruitment sites and euchromatic localization. *Embo J* **30**: 1012-1026.

Renauld H, Aparicio OM, Zierath PD, Billington BL, Chhablani SK, Gottschling DE. 1993. Silent domains are assembled continuously from the telomere and are defined by promoter distance and strength, and by SIR3 dosage. *Genes Dev* **7**: 1133-1145.

Simms TA, Dugas SL, Gremillion JC, Ibos ME, Dandurand MN, Toliver TT, Edwards DJ, Donze D. 2008. TFIIIC binding sites function as both heterochromatin barriers and chromatin insulators in Saccharomyces cerevisiae. *Eukaryot Cell* **7**: 2078-2086.

Stone EM, Pillus L. 1996. Activation of an MAP kinase cascade leads to Sir3p hyperphosphorylation and strengthens transcriptional silencing. *J Cell Biol* **135**: 571-583.

Terweij M, van Welsem T, van Deventer S, Verzijlbergen KF, Menendez-Benito V, Ontoso D, San-Segundo P, Neefjes J, van Leeuwen F. 2013. Recombination-induced tag exchange (RITE) cassette series to monitor protein dynamics in Saccharomyces cerevisiae. *G3 (Bethesda)* **3**: 1261-1272.

Teytelman L, Thurtle DM, Rine J, van Oudenaarden A. 2013. Highly expressed loci are vulnerable to misleading ChIP localization of multiple unrelated proteins. *Proc Natl Acad Sci U S A* **110**: 18602-18607.

Valcourt JR, Lemons JM, Haley EM, Kojima M, Demuren OO, Coller HA. 2012. Staying alive: metabolic adaptations to quiescence. *Cell Cycle* **11**: 1680-1696.

Verzijlbergen KF, Menendez-Benito V, van Welsem T, van Deventer SJ, Lindstrom DL, Ovaa H, Neefjes J, Gottschling DE, van Leeuwen F. 2010. Recombination-induced tag exchange to track old and new proteins. *Proc Natl Acad Sci U S A* **107**: 64-68.

Watanabe S, Radman-Livaja M, Rando OJ, Peterson CL. 2013. A histone acetylation switch regulates H2A.Z deposition by the SWR-C remodeling enzyme. *Science* **340**: 195-199.

Weiner A, Chen HV, Liu CL, Rahat A, Klien A, Soares L, Gudipati M, Pfeffner J, Regev A, Buratowski S et al. 2012. Systematic dissection of roles for chromatin regulators in a yeast stress response. *PLoS Biol* **10**: e1001369.

Weiner A, Hughes A, Yassour M, Rando OJ, Friedman N. 2010. High-resolution nucleosome mapping reveals transcription-dependent promoter packaging. *Genome Res* **20**: 90-100.

Ziane R, Camasses A, Radman-Livaja M. 2019. Mechanics of DNA Replication and Transcription Guide the Asymmetric Distribution of RNAPol2 and New Nucleosomes on Replicated Daughter Genomes. *bioRxiv*: 553669.

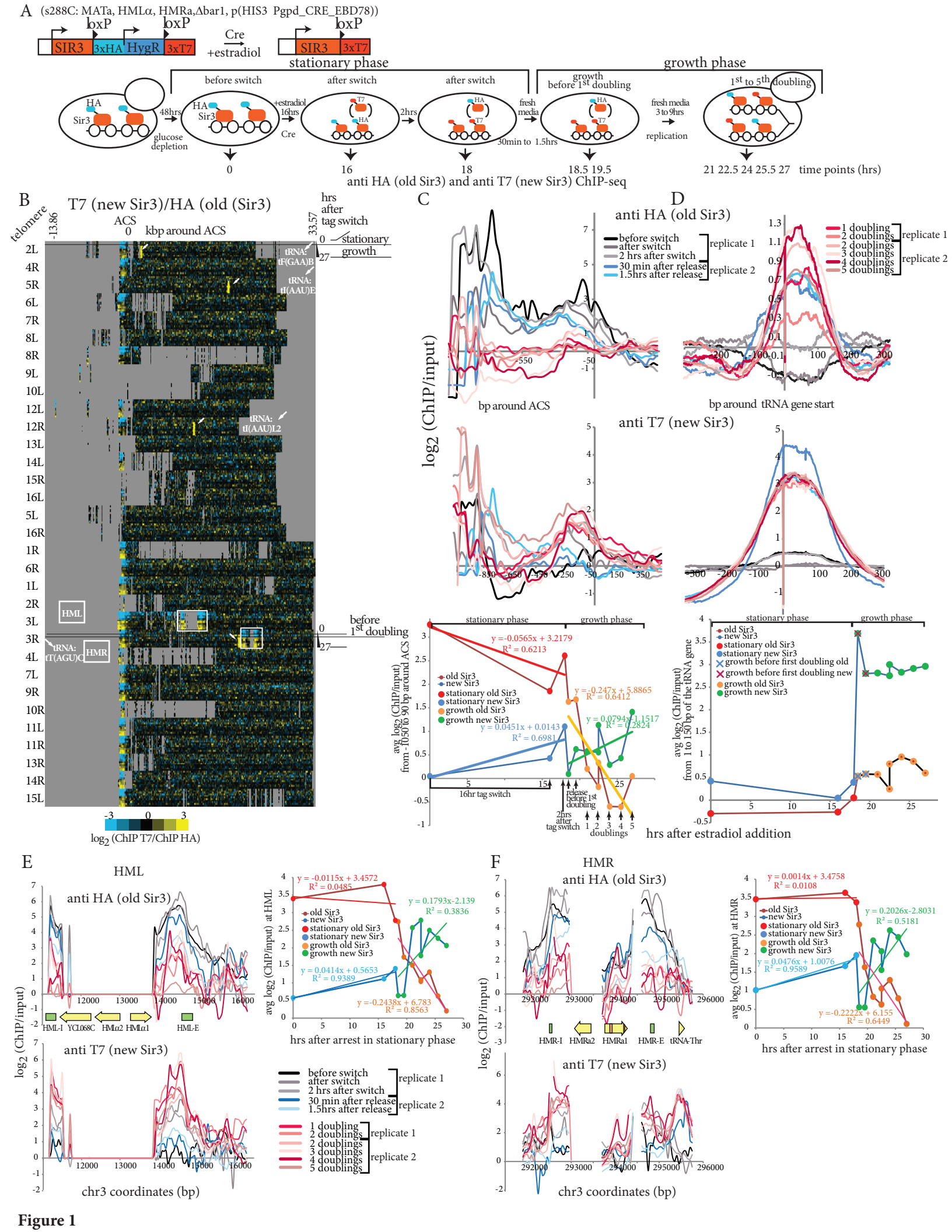
A
(s288C: MATa, HMLα, HMRa,Δbar1, p(HIS3 Pgpd_CRE_EBD78))
loxP
loxP
SIR3
3xHA
HygR
3xT7
Cre
+estradiol
loxP
SIR3
3xT7
stationary phase
growth phase
before switch
after switch
after switch
growth before 1st doubling
1st to 5th doubling
HA
Sir3
48hrs
glucose depletion
+estradiol 16hrs
Cre
T7
2hrs
fresh media
30min to 1.5hrs
fresh media 3 to 9hrs
replication
0
16
18
18.5 19.5
21 22.5 24 25.5 27 time points (hrs)
anti HA (old Sir3) and anti T7 (new Sir3) ChIP-seq
B
T7 (new Sir3)/HA (old Sir3)
telomere
-13.86
ACS
0
kbp around ACS
33.57
hrs after tag switch
stationary
growth
tRNA: tF(GAA)B
tRNA: tI(AAU)E
tRNA: tI(AAU)L2
HML
HMR
tRNA: tT(AGU)C
before 1st doubling
2L
4R
5R
6L
7R
8L
8R
9L
10L
12L
12R
13L
14L
15R
16L
5L
16R
1R
6R
1L
2R
3L
3R
4L
7L
9R
10R
11L
11R
13R
14R
15L
-3
0
3
log2 (ChIP T7/ChIP HA)
C
anti HA (old Sir3)
before switch
after switch
2 hrs after switch
30 min after release
1.5hrs after release
replicate 1
replicate 2
bp around ACS
log2 (ChIP/input)
anti T7 (new Sir3)
D
1 doubling
2 doublings
2 doublings
3 doublings
4 doublings
5 doublings
replicate 1
replicate 2
bp around tRNA gene start
stationary phase
growth phase
y = -0.0565x + 3.2179
R² = 0.6213
y = -0.247x + 5.8865
R² = 0.6412
y = 0.0794x - 1.1517
R² = 0.2824
y = 0.0451x + 0.0143
R² = 0.6981
old Sir3
new Sir3
stationary old Sir3
stationary new Sir3
growth old Sir3
growth new Sir3
avg log2 (ChIP/input) from -150 to 90 bp around ACS
16hr tag switch
release before 1st doubling
2hrs after tag switch
doublings
growth before first doubling old
growth before first doubling new
avg log2 (ChIP/input) from 1 to 150 bp of the tRNA gene
hrs after estradiol addition
E
HML
anti HA (old Sir3)
HML-I
YCL068C
HMLα2
HMLα1
HML-E
y = -0.0115x + 3.4572
R² = 0.0485
y = 0.1793x-2.139
R² = 0.3836
y = 0.0414x + 0.5653
R² = 0.9389
y = -0.2438x + 6.783
R² = 0.8563
avg log2 (ChIP/input) at HML
hrs after arrest in stationary phase
anti T7 (new Sir3)
chr3 coordinates (bp)
F
HMR
anti HA (old Sir3)
HMR-I
HMRa2
HMRa1
HMR-E
tRNA-Thr
y = 0.0014x + 3.4758
R² = 0.0108
y = 0.2026x-2.8031
R² = 0.5181
y = 0.0476x + 1.0076
R² = 0.9589
y = -0.2222x + 6.155
R² = 0.6449
avg log2 (ChIP/input) at HMR
hrs after arrest in stationary phase
anti T7 (new Sir3)
chr3 coordinates (bp)

Figure 1

Figure 1: A. Diagram of the Sir3 tag switch construct used in ChIP-seq experiments shown here (top left). Bottom: Experiment outline. Cells were arrested by glucose depletion before the tag switch, which is induced with estradiol addition to arrested cells (95% -98% of cells typically switch after a 16hr incubation). Cells were then released from arrest with addition of fresh media and allowed to grow for one to five doublings (monitored by OD measurements). Cell aliquots were fixed with 1% formaldehyde for 20min at times indicated below the diagrams and anti-HA and anti-T7 (polyclonal XXX) ChIPs were performed on sonicated chromatin. B. Heat map of new Sir3 (T7 tag) enrichment over old Sir3 (HA tag) during and after exit from quiescence, at all yeast telomeres (30kbp from chromosomes ends). Time points are aligned by the ARS Consensus Sequence (ACS) located in telomeric silencer regions, which are Sir complex nucleation sites at telomeres. White arrows show tRNA genes where new Sir3 binds after exit from quiescence. Silent mating type loci HML and HMR, on 3L and 3R, respectively, are framed with a white rectangle. Sir3 is enriched in a small 1kb region upstream of the ACS at all telomeres. Repetitive and unmapped regions are shown in grey. The HMLα reads have been eliminated as repetitive sequences during alignment to the reference genome which is MATα. C-D. Old (top) and new (middle) Sir3 enrichment around ACS averaged for all 32 telomeres (C) or tRNA genes averaged for all 274 genes (D) at indicated time points during the stationary and the renewed growth phases. The bottom panel shows average enrichment around the ACS (C) or tRNA genes (D) for old and new Sir3 over time. E-F. Old (top left) and new (bottom left) Sir3 enrichment at HML (E) and HMR (F) at indicated time points (same color code for E and F) during the stationary and the renewed growth phase. The right panel shows average enrichment over the entire silent mating type locus for old and new Sir3 over time.

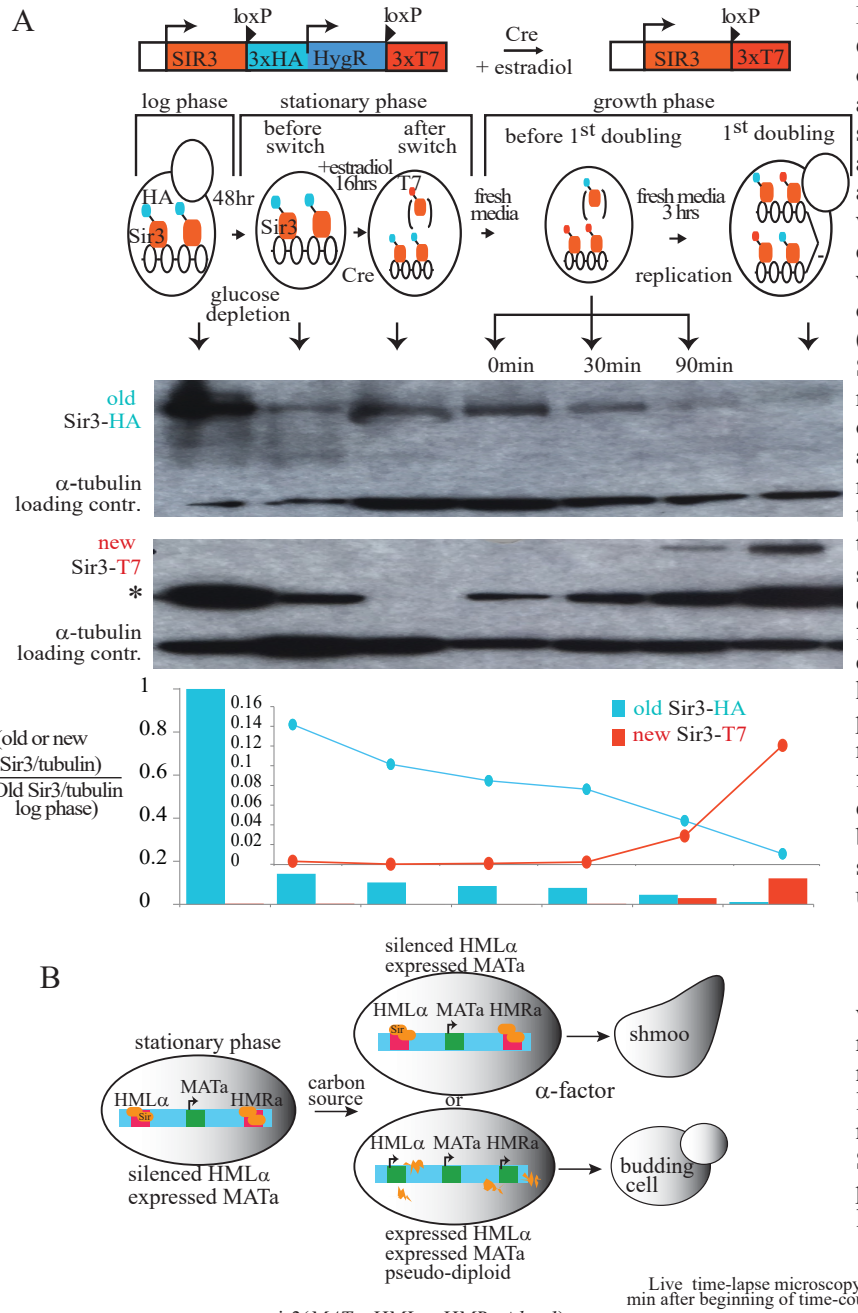

Figure 2: Heterochromatin is destabilized before the first division following exit from stationary phase. A. Western blot of old Sir3-HA (anti-HA antibody) and new Sir3-T7 (anti T7 antibody) from total cell extracts during and after release from stationary phase. The top panel shows the experimental outline and describes the timepoints shown in the blot (marked by arrows above the blot). * marks a non-specific band detected with the anti-T7 antibody. The graph below the blot shows the quantification of the bands from the blot. Sir3 band intensities were first normalized to the α-tubulin loading control and than divided by the normalized Sir3-HA intensity from midlog cells (bar graph). The line plot inset shows the same normalized Sir3-HA and Sir3-T7 band intensities for all timepoints after midlog. **B.** α-factor heterochromatin stability test. The diagram on top shows the expected response of MATa cells to α-factor added after release from stationary phase. If the Sir heterochromatic complex is unstable HMLα and HMRa will be transcribed along with MATa, thus creating pseudo-diploid cells that don't respond to α-factor and consequently do not become shmoo but start budding instead. The bottom panel shows examples of frames from a live cell imaging experiment that follows log phase cells (top), stationary phase cells in the first cell cycle after release (middle) or stationary phase cells that have undergone one cell division after release (bottom) in the presence of 0.2μg/ml α-factor 0 and 380min after the beginning of the time course. The bar graph on the right shows the fraction of budding cells in all cells (budding and shmoo) for each cell population. The p-values for the null-hypothesis between released stationary phase cells and log-phase cells shown above the bars are calculated from the Z score obtained using Z-test statistics with significance cutoff α=0.05:

$$Z=\frac{(p1-p2)-0}{\sqrt{p(1-p)((1/n1)+(1/n2))}}$$

where p1 and p2 are n(budding)/n(shmoos +budding) in cells released from stationary phase and log-phase cells respectively, n1 and n2 are n(shmoos+budding) in stationary phase and log-phase cells respectively and p is (n(budding)stationary + n(budding)midlog) / (n1+n2). **C.** α–factor test with the OE Sir3 strain which shmooes independently of Sir3 in the presence of α–factor because of the deletion of HML and MAT loci.

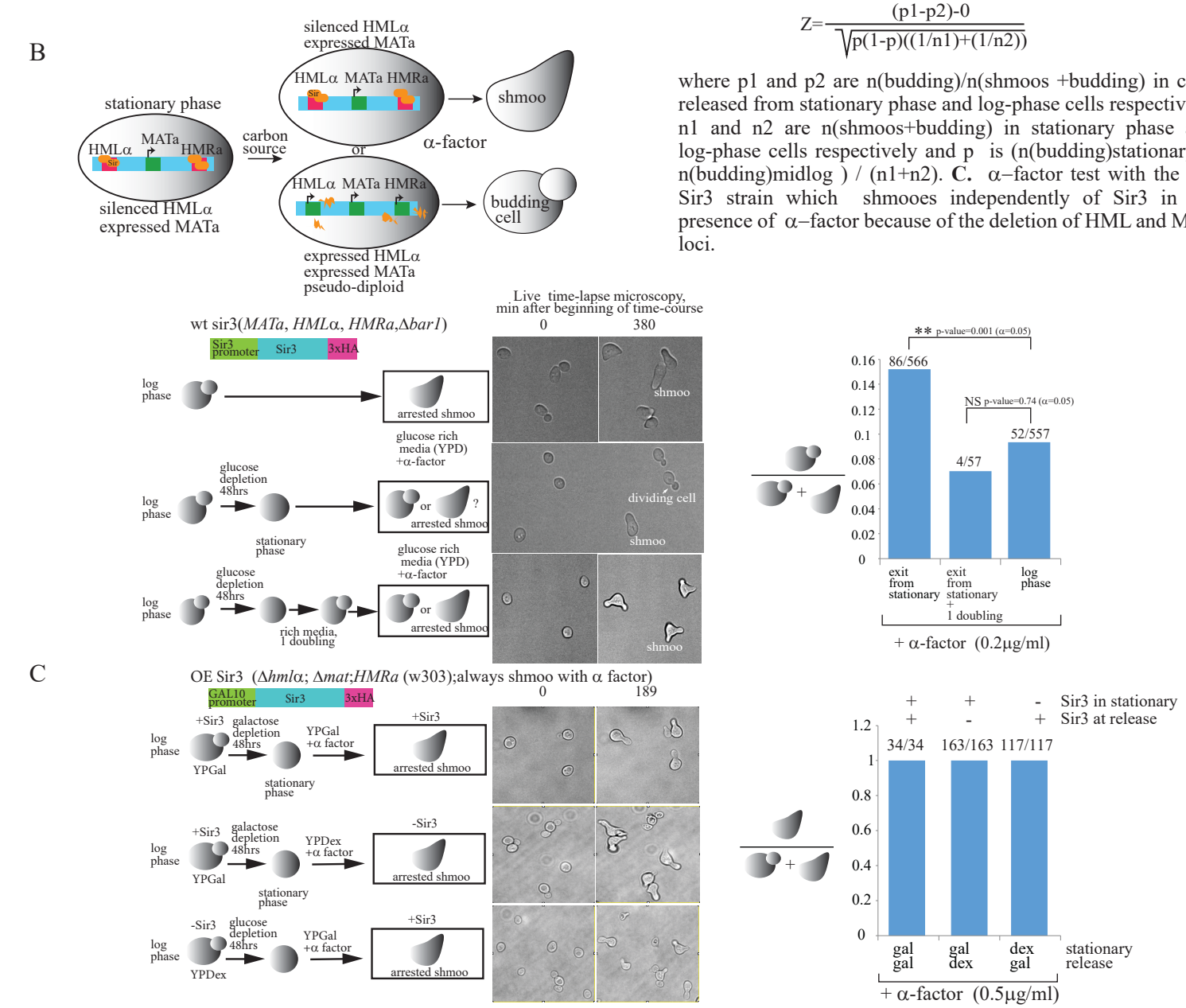

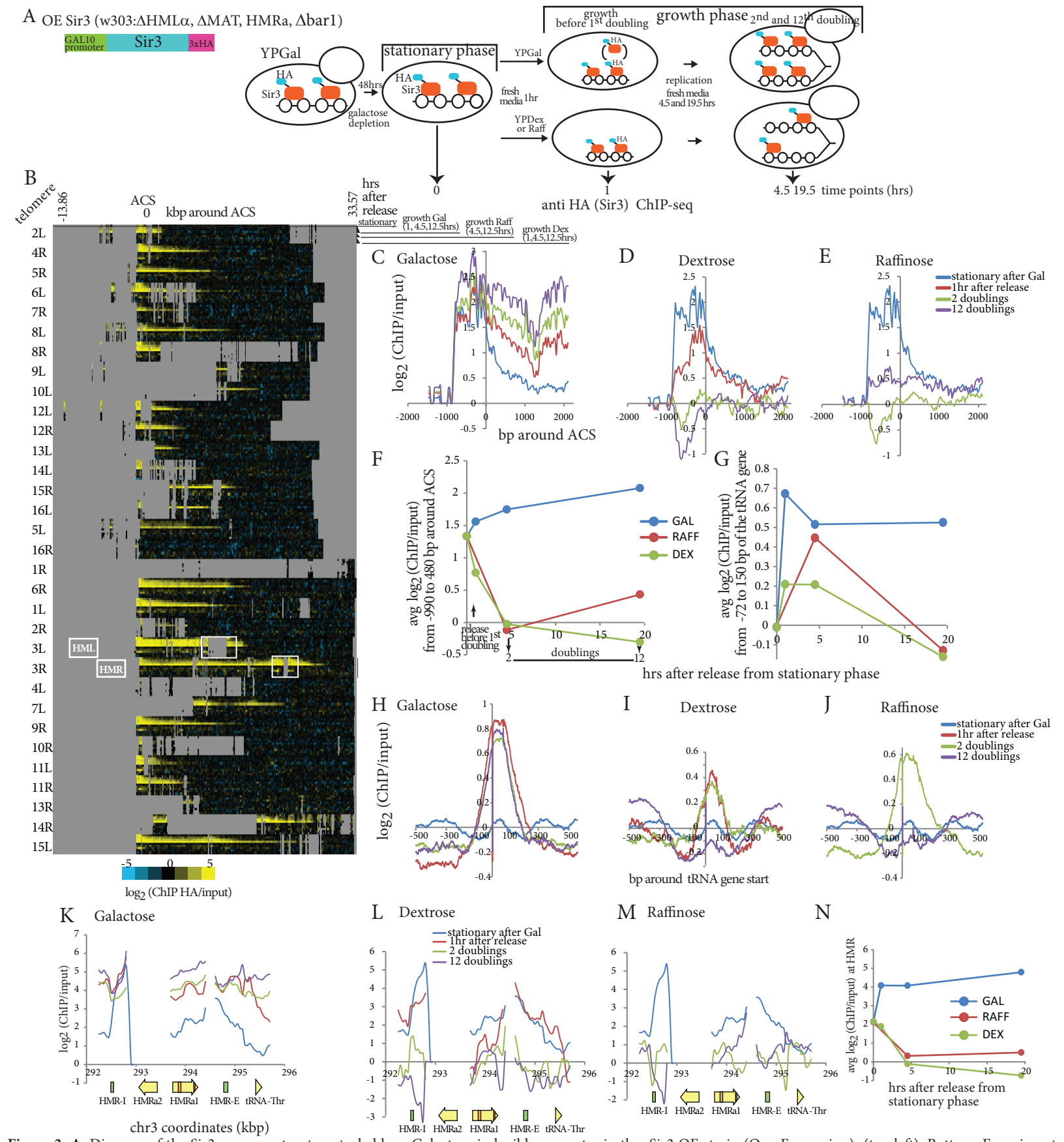

Figure 3: A. Diagram of the Sir3 gene construct controled by a Galactose inducible promoter in the Sir3 OE strain (OverExpression) (top left). Bottom: Experiment outline. Cells were arrested by galactose depletion, and released of fresh media with the indicated carbon source (2%) and allowed to grow for 2 and 12 doublings (monitored by OD measurements). Cell aliquots were fixed with 1% formaldehyde for 20min at times indicated below the diagrams and anti-HA ChIPs were performed on sonicated chromatin. **B**. Heat map of Sir3 (HA tag) enrichment over input during and after exit from quiescence, at all yeast telomeres (30kbp from chromosomes ends). Time points are aligned by the ARS Consensus Sequence (ACS) located in telomeric silencer regions, which are Sir complex nucleation sites at telomeres. Silent mating type loci HML (HML is deleted in this strain) and HMR, on 3L and 3R, respectively, are framed with a white rectangle. Repetitive and unmapped regions are shown in grey. **C-E**. Sir3 enrichment around ACS averaged for all 32 telomeres after release into Galactose- over expression of Sir3 (C), Dextrose- inhibition of Sir3 expression (D) or Raffinose- low Sir3 expression (E). **F-G.** Average Sir3 enrichment around the ACS (E) or tRNA genes (F) over time in indicated carbon sources. **H-J.** Average Sir3 enrichment at tRNA genes for all 274 genes after release into Galactose (H), Dextrose (I) or Raffinose (J). **K-M**. Sir3 enrichment at HMR after release into Galactose (K), Dextrose (L) or Raffinose (M). **N** Average Sir3 enrichment over the entire HMR over time .

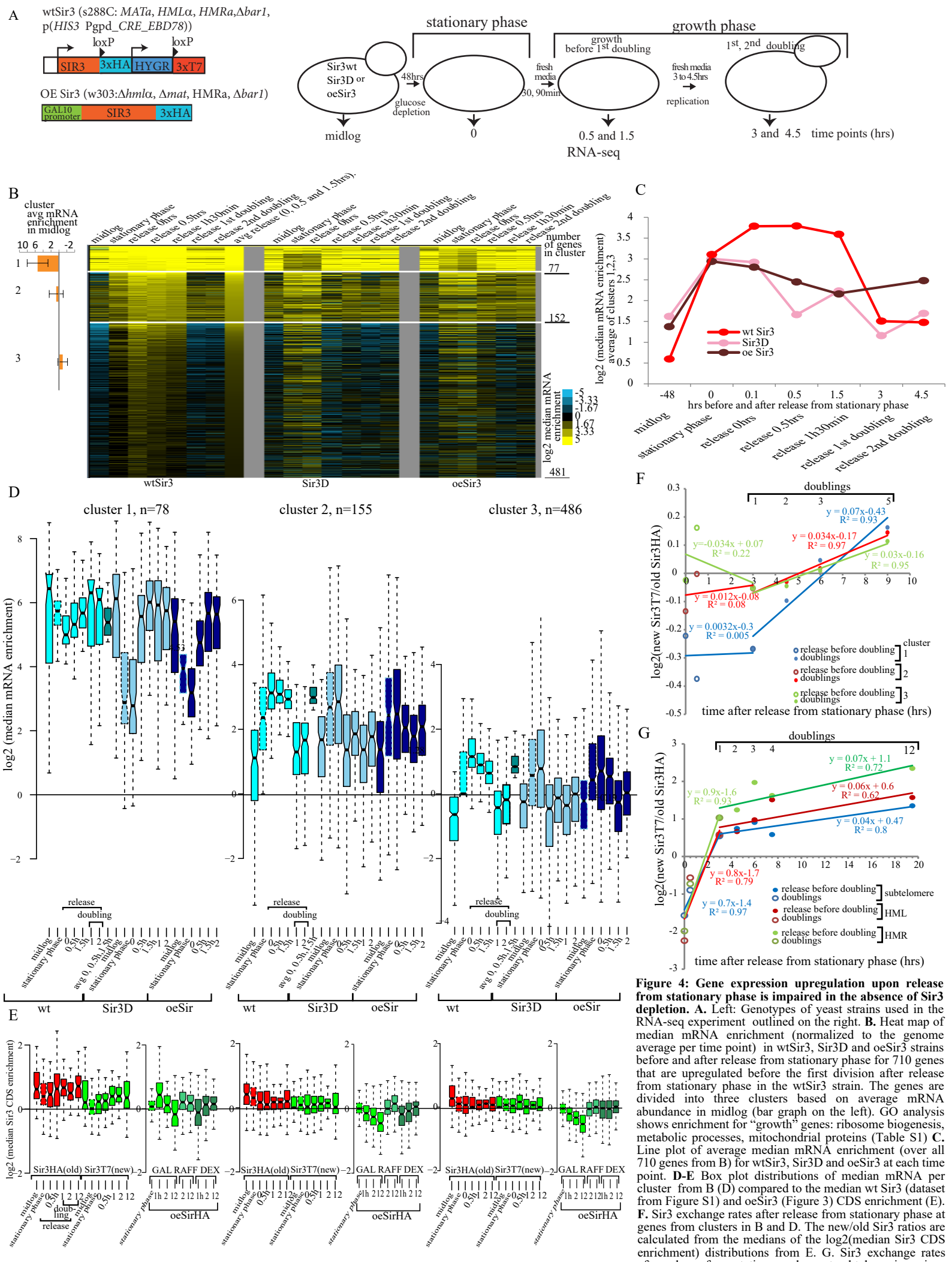

Figure 4: Gene expression upregulation upon release from stationary phase is impaired in the absence of Sir3 depletion. A. Left: Genotypes of yeast strains used in the RNA-seq experiment outlined on the right. **B.** Heat map of median mRNA enrichment (normalized to the genome average per time point) in wtSir3, Sir3D and oeSir3 strains before and after release from stationary phase for 710 genes that are upregulated before the first division after release from stationary phase in the wtSir3 strain. The genes are divided into three clusters based on average mRNA abundance in midlog (bar graph on the left). GO analysis shows enrichment for "growth" genes: ribosome biogenesis, metabolic processes, mitochondrial proteins (Table S1) **C.** Line plot of average median mRNA enrichment (over all 710 genes from B) for wtSir3, Sir3D and oeSir3 at each time point. **D-E** Box plot distributions of median mRNA per cluster from B (D) compared to the median wt Sir3 (dataset from Figure S1) and oeSir3 (Figure 3) CDS enrichment (E). **F.** Sir3 exchange rates after release from stationary phase at genes from clusters in B and D. The new/old Sir3 ratios are calculated from the medians of the log2(median Sir3 CDS enrichment) distributions from E. G. Sir3 exchange rates after release from stationary phase at subtelomeric regions and HMR and HML from Figure S1. The new/old Sir3 ratios are calculated from the average Sir3 enrichment shown in Figure S1.

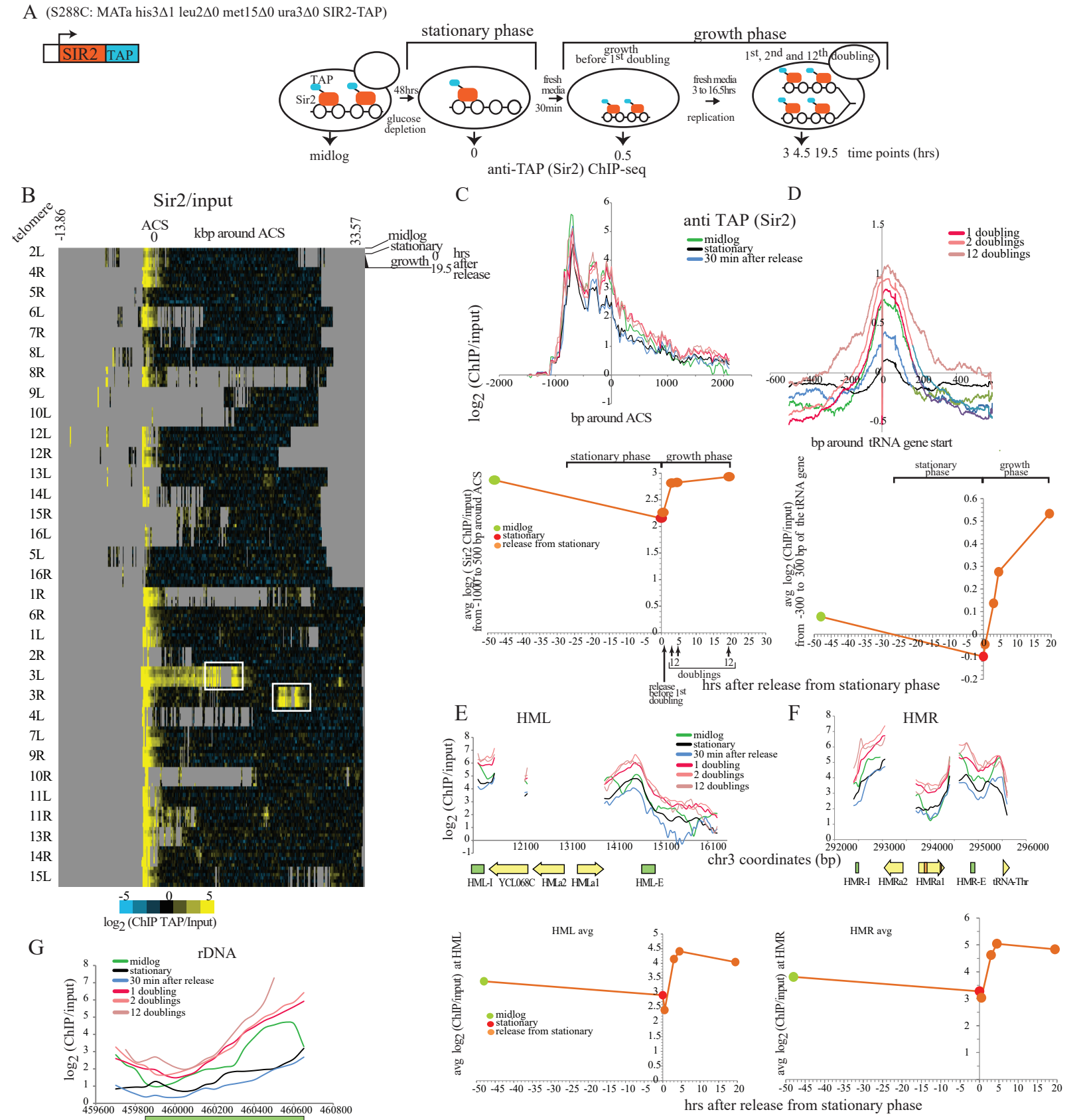

Figure 5: A. Diagram of the Sir2-TAP tag construct used in ChIP-seq experiments shown here (top left). Bottom: Experiment outline. Cells were grown for 48hrs until they reached stationary phase by glucose depletion . Cells were then released from arrest with addition of fresh media and allowed to grow for one to twelve doublings (monitored by OD measurements). Cell aliquots were fixed with 1% formaldehyde for 20min at times indicated below the diagrams and anti-TAP ChIPs were performed on sonicated chromatin. B. Heat map of Sir2 (TAP tag) enrichment over input during and after exit from quiescence, at all yeast telomeres (30kbp from chromosomes ends). Time points are aligned by the ARS Consensus Sequence (ACS) located in telomeric silencer regions i.e. Sir complex nucleation sites at telomeres. Silent mating type loci HML and HMR, on 3L and 3R, respectively, are framed with a white rectangle. Sir2 is enriched in a small 1kb region upstream of the ACS at all telomeres. Repetitive and unmapped regions are shown in grey. The HMLa reads have been eliminated as repetitive sequences during alignment to the reference genome which is MATa. C-D. Sir2 enrichment around ACS averaged for all 32 telomeres (C) or tRNA genes averaged for all 274 genes (D) at indicated time points during the stationary and the renewed growth phases. The bottom panel shows average enrichment around the ACS (C) or tRNA genes (D) for Sir2 over time. E-G. Sir2 enrichment at HML (E), HMR (F) and rDNA (G) (NTS1-2 is the non-transcribed region of the rDNA repeat between the 3' ETS and RDN5) at indicated time points during the stationary and the renewed growth phase. The bottom panel shows average enrichment over the entire silent mating type locus or rDNA for Sir2 over time.

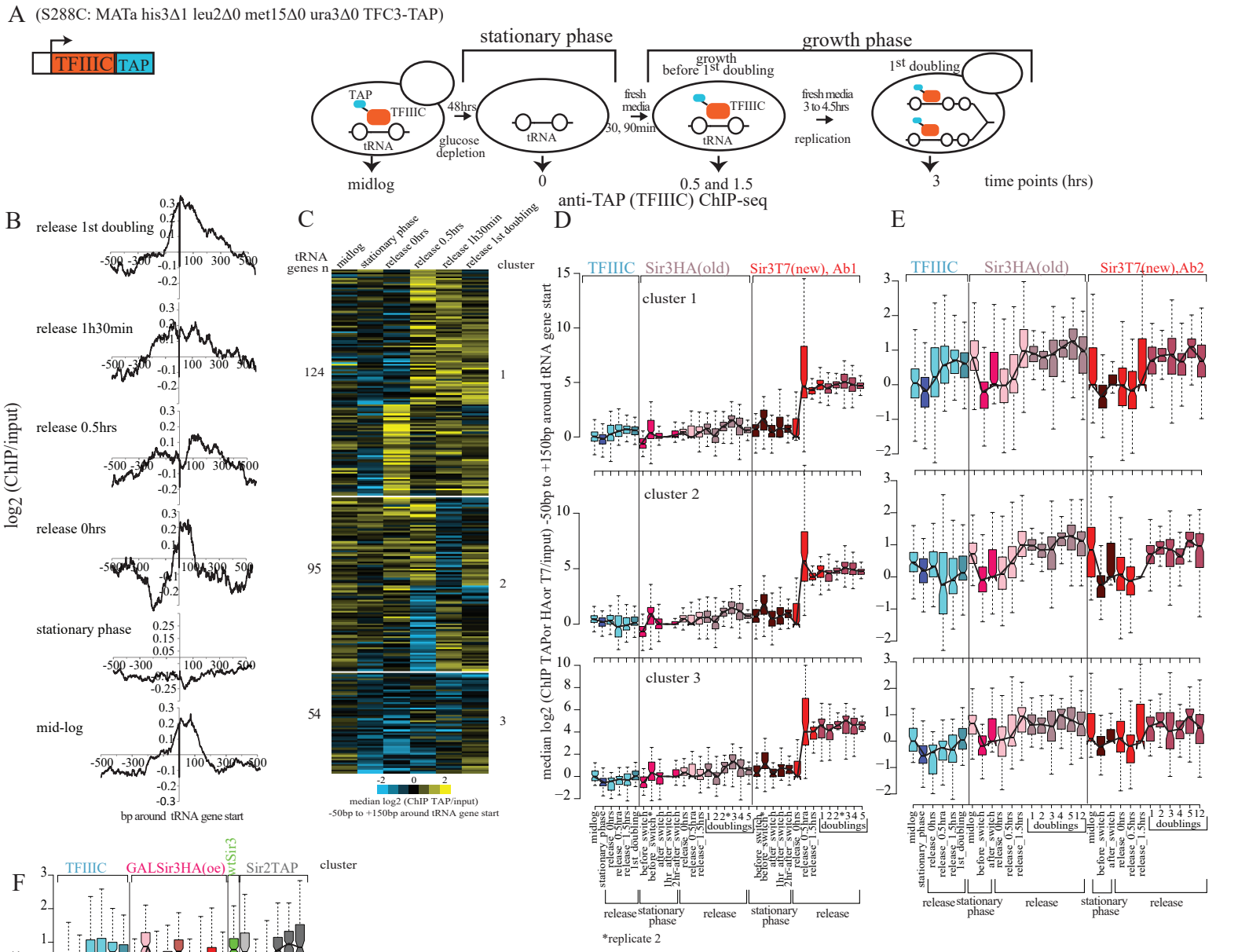

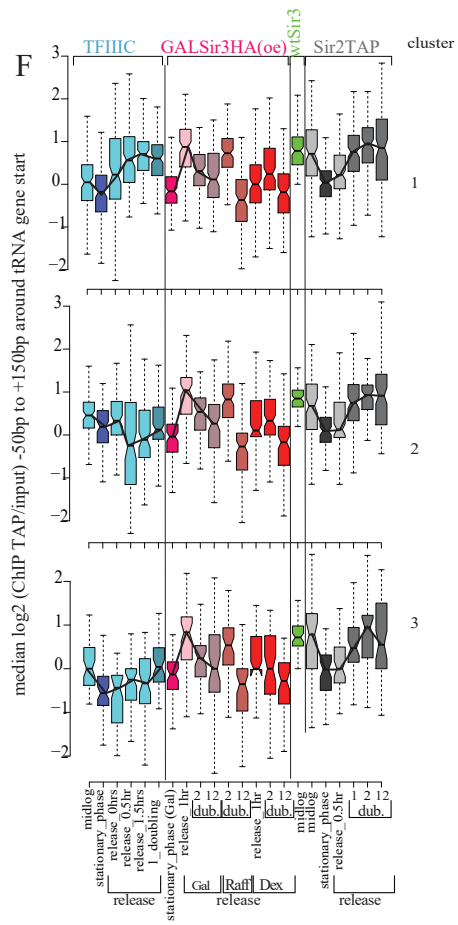

Figure 6: TFIIIC binding to tRNA genes upon release from stationary phase. A. Diagram of the TFC3-TAP tag construct used in ChIP-seq experiments shown here (top). Right: Experiment outline. Cells were grown for 48hrs until they reached stationary phase by glucose depletion . Cells were then released from arrest with addition of fresh media and allowed to grow for one to twelve doublings (monitored by OD measurements). Cell aliquots were fixed with 1% formaldehyde for 20min at times indicated below the diagrams and anti-TAP ChIPs were performed on sonicated chromatin. B. Average profiles of TFIIIC (TAP tag) enrichment over input at all 274 tRNA genes before, during and after exit from quiescence. C K-means clustering of median TFIIIC enrichment at tRNA genes (-50 to +150 bp around the start of the gene) at indicated timepoints (columns). Cluster 1: tRNA genes with increased TFIIIC binding after release; Cluster 2:tRNA genes with reduced TFIIIC binding after release; Cluster 3:low binding TFIIIC tRNA genes with slow recovery after release. D-F box plot distributions of median read density enrichment comparing TFIIIC binding to old(HA)/new(T7) Sir3 (D: Figure 1, polyclonal anti-T7; E: Figure S1, monoclonal anti-T7) , over-expressed Sir3 (Galactose inducible, Figure S2) and Sir2 (F, Figure 3) at tRNA genes from clusters shown in C. Sir3 and Sir2 binding is independent of TFIIIC binding (and consequently tRNA expression) since binding dynamics of Sir3 and Sir2 before and after stationary phase are the same for all three clusters from C: Sir3 and Sir2 are depleted from tRNA genes in stationary phase and rebind gradually before the first doubling after release and stay stably bound through at least 12 doublings. The polyclonal anti-T7 antibody (D, Figure 1) appears to have a much higher affinity for the T7 tag than the monoclonal anti-T7 used in Figure S1 (E), at least in the Sir3 configuration bound to tRNA genes since a difference between these two antibodies is not detected at telomeres and silent mating type loci (compare Figures 1 and S1). It is therefore difficult to judge wether binding of old Sir3 detectable even at 12 doublings after release comes from cells that have not undergone tag switch (about 2% of the initial population in stationary phase) or from a fraction of old Sir3 that has "survived" since the stationary phase. Sir3 binding is not a "tag" artefact as untagged "wt Sir3" (custom ant-Sir3 antibody, dataset from Radman-Livaja et al., 2011, EMBOJ.) (F) and old-Sir3 HA (E) have similar enrichment distributions in midlog cells.